J Neurophysiol 90: 2648–2659, 2003.
First published July 2, 2003; 10.1152/jn.00348.2003.

Spatial Tuning to Virtual Sounds in the Inferior Colliculus of the Guinea Pig

Susanne J. Sterbing,[1] Klaus Hartung,[2] and Klaus-Peter Hoffmann[1]
[1]*Department of Zoology and Neurobiology and* [2]*Institute of Communication Acoustics, Ruhr University, Bochum 44780, Germany*

Submitted 9 April 2003; accepted in final form 26 June 2003

Sterbing, Susanne J., Klaus Hartung, and Klaus-Peter Hoffman. Spatial tuning to virtual sounds in the inferior colliculus of the guinea pig. *J Neurophysiol* 90: 2648–2659, 2003. First published July 2, 2003; 10.1152/jn.00348.2003. How do neurons in the inferior colliculus (IC) encode the spatial location of sound? We have addressed this question using a virtual auditory environment. For this purpose, the individual head-related transfer functions (HRTFs) of 18 guinea pigs were measured under free-field conditions for 122 locations covering the upper hemisphere. From 257 neurons, 94% responded to the short (50-ms) white noise stimulus at 70 dB sound pressure level (SPL). Out of these neurons, 80% were spatially tuned with a receptive field that is smaller than a hemifield (at 70 dB). The remainder responded omnidirectionally or showed fractured receptive fields. The majority of the neurons preferred directions in the contralateral hemisphere. However, preference for front or rear positions and high elevations occurred frequently. For stimulation at 70 dB SPL, the average diameter of the receptive fields, based on half-maximal response, was less than a quarter of the upper hemisphere. Neurons that preferred frontal directions responded weakly or showed no response to posterior directions and vice versa. Hence, front/back discrimination is present at the single-neuron level in the IC. When nonindividual HRTFs were used to create the stimuli, the spatial receptive fields of most neurons became larger, split into several parts, changed position, or the response became omnidirectional. Variation of absolute sound intensity had little effect on the preferred directions of the neurons over a range of 20 to 40 dB above threshold. With increasing intensity, most receptive fields remained constant or expanded. Furthermore, we tested the influence of binaural decorrelation and stimulus bandwidth on spatial tuning. The vast majority of neurons with a low characteristic frequency ($<$2.5 kHz) lost spatial tuning under stimulation with binaurally uncorrelated noise, whereas high-frequency units were mostly unaffected. Most neurons that showed spatial tuning under broadband stimulation (white noise and 1 octave wide noise) turned omnidirectional when stimulated with 1/3 octave wide noise.

INTRODUCTION

External sounds are diffracted and partly shadowed by the head and body and then are further modified as they enter the external ear. Thus spectral modifications, which are specific with respect to the directions of the sound sources relative to the listener's head, are imposed on the incoming sound signals on their way to the eardrums. It is possible to measure these head-related transfer functions (HRTFs) by recording signals in the ear canal after presentation of sounds at different locations (for review, see Blauert 1996). Presenting sounds convolved with the HRTFs through earphones can result in percepts that are indistinguishable from the original external sounds. Thus these virtual acoustic space signals contain all information necessary for localization: interaural information [interaural level difference (ILD) and interaural time difference (ITD)] as well as monaural spectral cues.

Because the external ear can be described as a linear time-invariant system, the impulse response (in the time domain) or the transfer function (in the frequency domain) characterizes the alteration of a signal passing the external ear as a function of the angle of incidence, and can be replaced by electronic filters. Although virtual auditory environments are commonly used in human psychoacoustics (Blauert 1996; Wenzel et al. 1993; Wightman and Kistler 1989), only a few groups of neurobiologists have used this technique to characterize spatial selectivity in auditory neurons (Brugge et al. 1996; Delgutte et al. 1999; Keller et al. 1998). Brugge and coworkers used HRTFs measured in a single cat to measure the responses of neurons in the primary auditory cortex of other cats. They found that the spatial receptive fields were quite large and/or fractured (i.e., consisted of several fragments that were separated by unresponsive areas). However, localization performance in human listeners is best when their own set of HRTFs is used (Wenzel et al. 1993; Wightman and Kistler 1989), and can degrade markedly when another listener's HRTFs are used. Therefore in the present study, a virtual auditory environment based on the animals' own HRTFs was used to characterize the spatial tuning of neurons in the inferior colliculus (IC). The use of a virtual auditory environment avoids numerous problems associated with free-field stimulation. Head holders, electrode microdrives, and stereotaxic benches produce acoustic reflections and distortions. Furthermore, it is difficult to control for pinna position, which is a critical parameter for the internal representation of auditory space (cat: Young et al. 1996). Furthermore, a virtual auditory environment allows signal manipulations that are impossible with free-field stimulation (e.g., uncorrelated noise signals can be presented through the spatially correct HRTFs).

We chose the IC because it is an obligatory synaptic station for multiple brain stem pathways that originate in the cochlear nucleus (Cant 1982; Oliver and Morest 1984; Rockel and Jones 1973). Lesion studies suggest that the IC is involved in auditory space localization (e.g., Jenkins and Masterton 1982). Because most free-field studies presented only sound source positions along the horizontal plane and/or from the frontal hemisphere, little is known about the representation of elevation and positions of the posterior hemisphere in the IC. Many studies were performed at near-threshold sound pressure levels

Address for reprint requests and other correspondence: S. J. Sterbing, Department of Psychology, Vanderbilt University, 301 Wilson Hall, Nashville, TN 37203 (E-mail: S.Sterbing@vanderbilt.edu).

The costs of publication of this article were defrayed in part by the payment of page charges. The article must therefore be hereby marked "*advertisement*" in accordance with 18 U.S.C. Section 1734 solely to indicate this fact.

(SPLs) and/or narrow band or pure tone signals were used for stimulation. The receptive fields measured under this condition are mainly based on monaural pinna isoamplification contours that alone cannot provide the basis for the auditory space representation (e.g., Fuzessery and Pollak 1985; Moore et al. 1984). Consistent with this finding is that localization acuity decreases close to the auditory threshold (Inoue 2001; Su et al. 2000).

The aim of the present study was to investigate the representation of sound direction in the IC, a structure that is thought to be a major integration center of signals preprocessed by lower, brain stem pathways (Oliver et al. 1997). Because spectral information is essential for localization along the medial plane, we stimulated from directions covering the entire upper hemisphere. The receptive fields measured with the method of virtual sound source generation described here are comparable to those obtained under free-field stimulation because a direct comparison of the virtual acoustic space and the free-field stimuli recorded at the eardrum revealed no significant differences for most sound source positions (see RESULTS, Keller et al. 1998). As in humans (Wenzel et al. 1993), the individuality of the pinna structure in the guinea pig made it necessary to use individual HRTFs. Furthermore, we examined how manipulations of the virtual auditory environment (use of the HRTFs of another individual, decorrelation, SPL, spectral bandwidth) influenced spatial tuning of single neurons.

METHODS

Generation of the virtual auditory environment

RECORDING OF THE HEAD-RELATED TRANSFER FUNCTIONS. The HRTFs were measured at the Institute of Communication Acoustics at the Ruhr University Bochum. The guinea pigs were anesthetized with a single dose of ketamine hydrochloride [Ketavet, 100 mg/kg body weight, intramuscularly (im)] and xylazine (Rompun, 2%, 1.5 ml/kg body weight, im). Atropine sulfate (0.06 mg/kg body weight) was injected subcutaneously to avoid hypersalivation. For HRTF measurement, a jaw holder was used to fix the position of the head so that the eyes and ears were in the horizontal plane. The exact positions of the animal's body axis, head, and ears were measured using 3 laser pointers. The animal was placed in the prone position on a turntable that was slightly smaller than the animal, so that no additional reflections were caused by it. This turntable was placed in the center of an anechoic room (about $5 \times 5 \times 5$ m, absorber: G&H Isover SPS2, low-end cutoff frequency: 110 Hz). Miniature microphones (Knowles 3046) were positioned in both ears, well within the straight portion of the ear canal, several millimeters behind the ear canal opening. The microphones filled the whole diameter of the ear canal and blocked the incoming sound waves from traveling further to the tympanum. With proper equalization these measurements can re-create the sound spectrum at the tympanum (Kulkarni and Colburn 1998). The HRTFs measured at the tympanum can be separated into 2 terms: one that varies with direction of incidence, and another term that contains the nondirectional transfer function of the ear canal (e.g., Hammershøi and Møller 1996). The directional part of the HRTF can be measured at a distance of a few millimeters from the entrance of the blocked ear canal. If the sound pressure at this position matches the sound pressure of free-field stimulation, the sound pressure at the eardrum is the same as in the free field.

We measured HRTFs for 122 directions of the upper hemisphere using 11 loudspeakers that were mounted on a vertically oriented arc ranging from −10 to 90° in 10° steps. After measuring HRTFs for all the elevations for one azimuth, the table was turned clockwise in 15° steps to cover the 360° of azimuth. To keep the density of measured directions constant, not all elevations of each azimuth were tested. After the HRTF measurements the animals were allowed to recover for ≥12 h. The first 3 measurements (0° azimuth at −10, 0, and 10° elevation) were repeated to make sure that the microphone position did not change during the 1-h measurement session. To confirm that the HRTFs derived from our microphone position contained all of the directional information, a probe tube was attached to the microphone and the tip of the probe tube was placed at different distances from the tympanic membrane. With the probe tubes located at the eardrums, the presentation of sound through the earphones was compared with a free-field loudspeaker presentation (see RESULTS).

In contrast to many other mammalian species, domestic guinea pigs do not move their pinnae during localization. Domestic guinea pigs have floppy ears, and during orientation movements to sound, they usually turn their head and/or body (unpublished observation). The guinea pigs were anesthetized during the HRTF recording. We found no obvious differences between the pinna position of the alert or anesthetized animal. However, it cannot be ruled out entirely that some subtle changes of pinna position occurred as a result of anesthesia (e.g., changes of muscle tone), but these changes were then the same both for the HRTF measurement and the electrophysiological experiment because the same anesthesia was used for both procedures. For these reasons, we felt it unnecessary to measure HRTFs at different pinna positions.

To acquire HRTFs, a random-phase noise sequence was used as test signal. Random-phase noise (RPN) has a flat amplitude spectrum and random-phase spectrum, which is uniformly distributed between −pi and +pi. The RPN was generated digitally [AP2, Tucker-Davis Technologies (TDT)] in the frequency domain by setting the amplitude value at each of the 2,048 frequency bins to one and filling the phase values at each bin with the output of a pseudorandom number generator. This sequence was transformed into the time domain using the inverse, discrete Fourier transform that results in a random-phase noise burst with 4,096 samples. This burst, which was repeated 100 times for each stimulus direction, was converted to an analog voltage (sampling frequency 50 kHz, TDT PD1), low-pass filtered (TDT FT6, corner frequency: 20 kHz), and then power-amplified (Sony TA–F450D) to a SPL of about 70 dB in the anechoic chamber (Bruel & Kjaer 2209 SPL meter) when played over one of the 11 individually equalized loudspeakers.

The signals picked up by the microphone were amplified (TDT MA2), low-pass filtered (TDT FT 6, corner frequency: 20 kHz), digitized (sampling rate: 50 kHz, TDT PD1), and then averaged in synchrony with the 100 times–repeated RPN burst (TDT AP2). Repeating the emitted noise bursts and the synchronous averaging of the response sequence improves the signal-to-noise ratio by eliminating the influence of extraneous noise, which is uncorrelated with the RPN sequence. The raw transfer function from the output of the D/A to the input of the A/D converter was derived by dividing the discrete Fourier transform of the response sequence by the discrete Fourier transform of the RPN sequence. This signal contains the head-related impulse response and distortions caused by unavoidable reflections and noise in the room that are caused, for example, by the steel net floor that allows persons to enter the room. These distortions were removed by windowing this signal in the time domain with a 128 samples–wide rectangular window. The optimal window position was determined by progressively sliding the window across the impulse response and by calculating the energy inside the window for each position. The position for which the energy first reaches a threshold of 90% of the maximal energy was chosen as the starting point of the window. This window size is sufficient, because the energy–time curve [20 log (envelope)] of the impulse response is reduced by more than 60 dB after 128 samples for all directions. The resulting impulse response/transfer function contains the directional characteristics of the head and pinna, filtered with the transfer functions of the loudspeakers and the microphones. The influence of the loudspeakers was removed by convolving the impulse response of the transfer function

with the impulse response of the inverse loudspeaker transfer function. The coefficients of the inverse filter (FIR-Filter, 512 coefficients) were calculated using a least-squares approximation (Proakis and Manolakis 1982). The error of the equalization, defined as the log ratio between the ideal and the realized filter, is <1 dB for all frequencies between 0.11 and 16 kHz.

EARPHONE MEASUREMENT AND CALIBRATION. These reflection-free, raw transfer functions must be compensated for the influence of the earphones coupled to the ear canal. This was done by measuring the transfer function from the earphone to the microphone in the ear canal and then filtering the raw HRTFs with the inverse transfer functions. The microphones were left in the same position as for the HRTF measurement and the tips of the tubes of the custom-made earphones (transducers: Beyer DT911) were positioned at the entrance to the ear canal. Because the HRTFs are calibrated by this measurement, the position of the earphone must be the same as when delivering the virtual sound sources. This was achieved by attaching the earphones to a stereotaxic frame, which allowed us to reposition them with an error of $<1°$. The transfer function from the earphones to the microphone was measured using the same procedure as described above. For the analysis of the HRTFs, the transfer function without the influence of the microphones and the loudspeakers is required. Therefore we measured the transfer function from each loudspeaker and equalized the measured HRTFs with the inverse transfer function of the respective loudspeaker.

Experimental procedure

ANIMALS. The pigmented guinea pigs ($n = 18$) were bred in the Department of Neuroethology at the University of Münster, Germany, and housed in the Department of Zoology and Neurobiology at the Ruhr University, Bochum. Their ages ranged from 4 to 6 mo. All animals had normal appearing external and middle ears.

SURGERY. Surgery and electrophysiological experiments were performed at the Department of Zoology and Neurobiology at the Ruhr University, Bochum. For surgery and neural recordings, the guinea pigs were anesthetized with the same drug regimen used in the HRTF measurement. Lidocaine was applied topically for analgesia. During the recordings, the guinea pigs metabolized the ketamine increasingly faster, so that the dose for maintaining anesthesia was increased every hour from 50 to 100 mg/kg ketamine after about 6 h. This procedure kept the animal in a light anesthetic state throughout the neural recordings (breathing rate was monitored). Animals were maintained at a rectal temperature of 38°C using a heating pad. After exposing the skull, a metal bolt was fixed to the bregma with histoacryl and dental cement and used to fix the position of the head. Holes of about 500 μm in diameter were drilled into the skull to allow microelectrode recordings from neurons in the left inferior colliculus. A second hole was made in the contralateral frontal skull for a silver-wire reference electrode.

ACOUSTIC STIMULATION AND ELECTROPHYSIOLOGICAL RECORDINGS. The guinea pigs were placed in a soundproof chamber (dimensions: $1 \times 1 \times 1.10$ m). Once a single-unit response was isolated, broadband virtual sounds (frozen Gaussian noise from 200 Hz to 16 kHz, 50-ms duration, 5-ms rise/fall time) from 122 directions of the entire upper hemisphere were presented by individually calibrated earphones to the animal in a pseudorandom order. After each of the 122 positions was tested once, this procedure was repeated 4 more times, leading to a total of 610 trials for one measurement of a spatial receptive field. For a subset of neurons we compared the responses under stimulation with correlated versus uncorrelated noise. For the uncorrelated stimulus, a different noise source was presented to each ear. This resulted in a signal that did not contain any low-frequency ITD information, but included all ILD cues and monaural spectral cues. For the correlated stimulus, the noise was exactly the same. With this test, we studied whether the neurons were sensitive to the fine structure of the noise signal. The SPL before convolution with the HRTFs was 80 dB. The sound pressure at the eardrum varies with sound source incidence and with frequency, caused by the filtering by the head and pinna. Thus it is unnecessary to equalize the SPL for these factors because the same happens under free-field stimulation.

The single-neuron responses in the central nucleus of the inferior colliculus (ICc) of the guinea pigs were recorded along 56 dorsoventrally oriented tracks in 18 animals. Glass micropipettes, filled with 3 M KCl, served as recording electrodes (impedance: about 3–10 MΩ). Spike times were acquired using a custom-built timer board, and the counts per stimulus were displayed on-line by the recording software. Frequency tuning curves and binaural characteristics of the neurons were also measured using tonal stimulation. The last penetration in each animal was made with a tungsten/iridium electrode to make electrolytic lesions (6 μA/2 min). The lesions served as benchmarks to make a 3D reconstruction of the recording sites. Brains were fixed by immersion in buffered formaldehyde solution (8%) for 3 wk, cryoprotected with 30% sucrose, sectioned (50 μm) with a cryostat in the transverse plane, and then stained with cresyl violet. All surgical, experimental, and euthanasia procedures were carried out in accordance with the European Communities Council Directive of November 24, 1986 (86/609/EEC) regarding the care and use of animals for experimental procedures, and were approved by the district government (26.8720) and the grant application agency (DFG grant Ho 450/23-1-347).

STATISTICS. The assessment of spatial tuning was based on a comparison of spike counts with respect to the latency of the unit under study. We found that latency often varied with sound source incidence. So as not to lose spikes, we adjusted the time window of analysis based on the directions that gave the shortest and longest latencies. To analyze and visualize the spatial tuning, the neuronal responses were processed by testing the number of spikes for each sound source direction against neighboring directions within a 17° range using the Kruskal–Wallis test (MATLAB version 5.3, statistics toolbox). If the difference between the direction under test and the neighboring directions was significant, the spike count of this direction was used for further analysis. If a direction failed this test, the median spike count of the direction under test and the neighbor directions was used. This procedure works like an adaptive median filter. The degree of smoothing is dependent on the local signal-to-noise ratio of the neuronal response. If the difference of the median firing rate between 2 neighboring positions is significant, there is no smoothing at all. If the difference is not significant, there would be smoothing, but only if the spike rate at the observed position differs greatly between the 5 trials. In our preparation this was only rarely the case. The size of the spatial receptive field was calculated on the basis of half-maximal response. The sound source direction that elicited the maximal spike count was defined as "best direction." For neurons with a plateaulike receptive field, the geometric center of the receptive field was chosen as the best direction. A receptive field was regarded as fractured if the half-maximal response contour showed more than one discrete region. The plots of the spatial tuning were calculated applying spherical spline interpolation (for details, see Hartung et al. 1999). For visualization in Cartesian coordinates we used a standard "Mercator"-like projection.

RESULTS

Head-related transfer functions

The HRTFs of all the guinea pigs showed asymmetries between the left and the right ear. This asymmetry was most prominent at high frequencies, and was found for both the standard microphone position at some distance to the tympanum (blocked ear canal) and the probe tube measurement directly at the eardrum. Thus it is unlikely that the asymmetry

is caused by different microphone positions. Calculation of the directional transfer function using the method of Kistler and Wightman (1992) also confirmed that the HRTFs were different for the left and right ears. The shapes of iso-interaural level difference (ILD) and iso-interaural time difference (ITD) contours varied with frequency. These contours were different for the same frequency and had an asymmetric shape relative to the frontal plane. The maximum ILD was 20 dB and the maximum ITD was 330 μs for low frequencies ($<$1.6 kHz). The ITDs were calculated by filtering the left and right head-related impulse responses with 1/3 octave band-pass filters. The envelopes of the 2 band-pass signals were systematically shifted and the maximal correlation defined the ITD value for the respective 1/3 octave band.

The HRTF measurements were highly reproducible. Figure 1*a* displays the difference between 5 measurements where the animal was turned to 90° azimuth and 0° elevation, the microphones were inserted, the HRTFs were measured, and then the microphones were removed. This procedure was repeated 5 times. The HRTFs differed by less than $\pm$1 dB for frequencies below 10 kHz, and by no greater than $\pm$4 dB for frequencies above 10 kHz. The HRTFs between animals showed considerable variability. Figure 1*b* displays the deviation of the individually measured HRTF at 90° azimuth and 0° elevation for 9 animals from the mean HRTF for this direction. The maximal difference was 35 dB (arrow). Hence, the interindividual differences (Fig. 1*b*) were much greater than the intra-individual differences (Fig. 1*a*).

To determine that the virtual auditory environment provides the auditory system with realistic information, we compared the frequency response and amplitude of both free-field and virtual sound source stimulation at the eardrum. The signal at the eardrum was measured with a Knowles microphone fitted with a small probe. It turned out that the difference for 106 of the 122 tested directions was $<$2 dB, and for the 16 "worst" matching directions, 3 dB. Figure 1*c* displays the deviation between free-field and virtual environment stimulation for a frontal direction (0° azimuth, 0° elevation) and Fig. 1*d* shows the difference for the 16 "worst" directions.

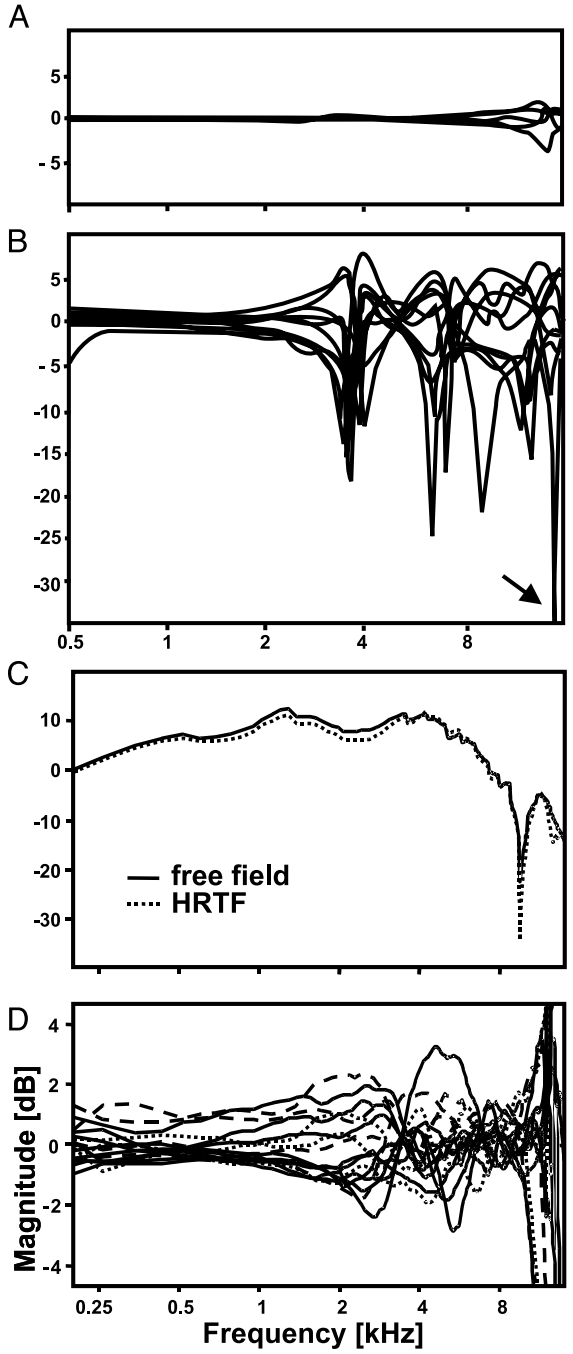

FIG. 1. Head-related transfer functions (HRTFs). *a*: deviation from mean for HRTFs at 90° azimuth and 0° elevation measured in one animal after reinsertion (5 times) of microphone. Difference is $<$2 dB for frequencies $\leq$10 kHz and $<$4 dB for frequencies $\leq$16 kHz. *b*: deviation from mean for HRTFs at 90° azimuth and 0° elevation measured in 9 different guinea pigs. Note that difference is $\leq$35 dB (arrow). *c*: transfer functions measured at eardrum for 0° azimuth and 0° elevation; dotted line: HRTF; solid line: free-field transfer function. *d*: difference between free-field transfer function and HRTF for 16 worst-matching directions. Difference is $<$3 dB for frequencies $\leq$10 kHz, and 4 dB for higher frequencies. For remaining 106 directions, difference was smaller than 2 dB.

Monaural cues

The directivity for the left and the right ear varied with frequency. For low frequencies (e.g., 0.5 kHz) the directional variation spanned only a few dB (Fig. 2*a*, *top panel*), with increasing frequency, this variation increased up to 15 dB. Figure 2*a* shows the isolevel contours for the left ear of one animal at 3 center frequencies of 1/3 octave bands. Note that the sound source direction that shows the greatest gain in level (i.e., the "acoustic axis") varies with frequency. Figure 2*b* summarizes the frequency-dependent shift of the acoustic axis for 7 animals. The mean position of the acoustic axis is indicated by a dot, the ellipses mark the SE. The numbers indicate the center frequency of each 1/3 octave band. Note that the acoustic axis was found at about 25° azimuth and 40° elevation for very low frequencies (0.2–0.3 kHz), at 70–80° azimuth and 20–40° elevation for frequencies between 1 and 2 kHz, low at the horizon for 5–10 kHz, and finally high in the front (10° azimuth, 70° elevation) for the highest frequencies tested.

Interaural cues

The ratio of the HRTFs of the left and right ear for the same direction is termed the *interaural transfer function*. From the interaural transfer function the ILD can be derived. The max-

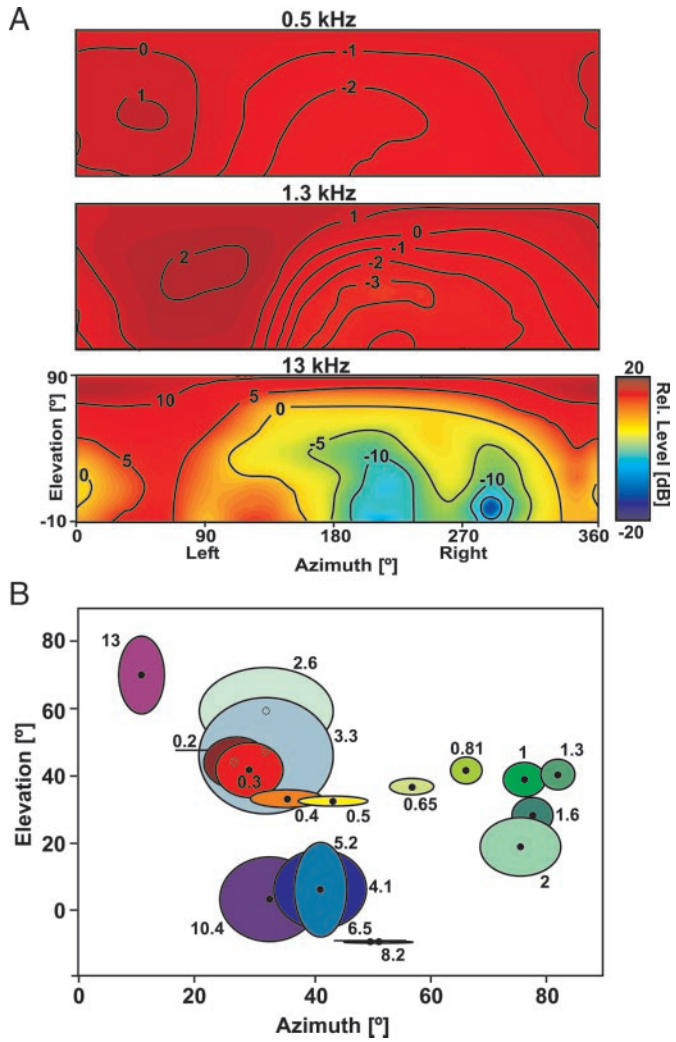

FIG. 2. Acoustic axis. *a*: isolevel contours at left ear for 3 frequency bands centered at 0.5, 1.3, and 13 kHz. Sound directions that produce same intensity are connected by contours, and marked with numbers indicating relative level in dB. Red areas indicate high relative level; green and blue areas, low relative level. *b*: average positions of highest relative levels (acoustic axis) for 7 animals. Dots mark mean, ellipses SE, for every frequency band. Numbers indicate center frequencies of bands. Note that average acoustic axis of guinea pig varies with frequency.

imum ILD was 15 to 20 dB. We estimated the maximal ITD for each 1/3 octave band ≤1.6 kHz by cross-correlating the HRTFs at each ear and found that it ranged ≤330 μs as a function of frequency. Figure 3 shows the maximum ITD for 30, 60, and 90° azimuth at 0° elevation. For 90° azimuth (sound from the side), we found the maximum of 330 μs at 400 and 500 Hz.

Frequency sampling and first-spike latencies

The penetrations covered a large proportion of the volume of the inferior colliculus. The histological reconstruction indicated that the recording sites were located in the central nucleus of the inferior colliculus according to the parcellation of Malmierca et al. (1995) for the guinea pig. The characteristic frequency of the neurons was determined using monaural tonal stimulation of the contralateral ear at different SPLs down to threshold. Only 6 neurons did not respond to tones. Only neurons with a characteristic frequency (CF) lower than 16 kHz were tested for spatial tuning because the measured transfer function of the Knowles microphones used to measure the HRTFs showed insufficient energy at higher frequencies. The lowest CF in the sample was 0.2 kHz. Although the first-spike latency to contralateral tones, presented by insertional earphone, was on average 10.9 ms (7.5–26.6 ms), the latency to the white noise stimulus, filtered with the HRTFs, was considerably longer: 19.6 ms (11.8–28.9 ms). For the broadband signal, many neurons displayed an early phase of inhibition, indicated by a reduction in spikes compared with the spontaneous activity, before they produced the spatially selective spikes (e.g., Fig. 4*d*). The onset of this inhibition could not be determined for all neurons because many were not spontaneously active. Thus the value for latency does not include this early phase of inhibition. The first-spike latency also varied with sound source incidence. On average the latency difference between the responses to preferred and nonpreferred positions was 4.7 ms (2.1–9.5 ms). Figure 4 shows spike-raster displays of 4 sample neurons for the white noise stimulus, filtered with the HRTFs.

Tuning to virtual sound sources

We recorded 257 single units under virtual sound source stimulation, of which 94% responded to the broadband test signal ($n = 242$). Each sound source direction (122 directions) was tested 5 times for a total of 610 stimuli per neuron. Out of the 242 responding neurons, 193 (80%) showed unfractured RFs covering half of the upper hemisphere or less (Kruskal–Wallis test: see METHODS). Figure 5 shows the spatial receptive field of 4 neurons, each tuned to a different sound direction. Most neurons had restricted spatial response areas, which covered less than an octant (quarter of the upper hemisphere). Only few neurons were classified as hemifield sensitive. Preference for rear directions and tuning to high elevations were also observed.

Distribution of best directions

To quantify the distribution of preferred azimuth, we divided the 122 stimulus directions into back and front, and contralat-

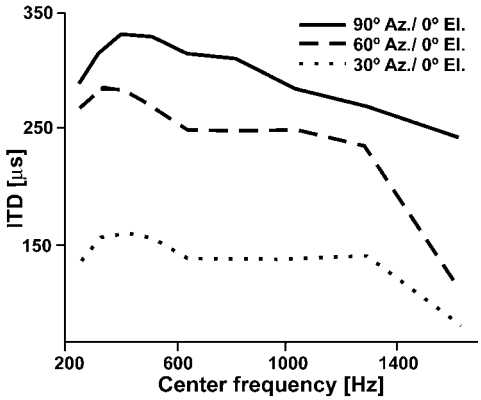

FIG. 3. Physiological range of interaural time difference (ITD). Maximum ITD was calculated for 1/3 octave bands by cross-correlating HRTFs for both ears. Maximum ITD is plotted for 3 sound source directions, 30, 60, and 90° azimuth at 0° elevation vs. center frequency of each 1/3 octave band. For 90° azimuth (i.e., sound source was located at side of head), highest ITD value was 330 μs.

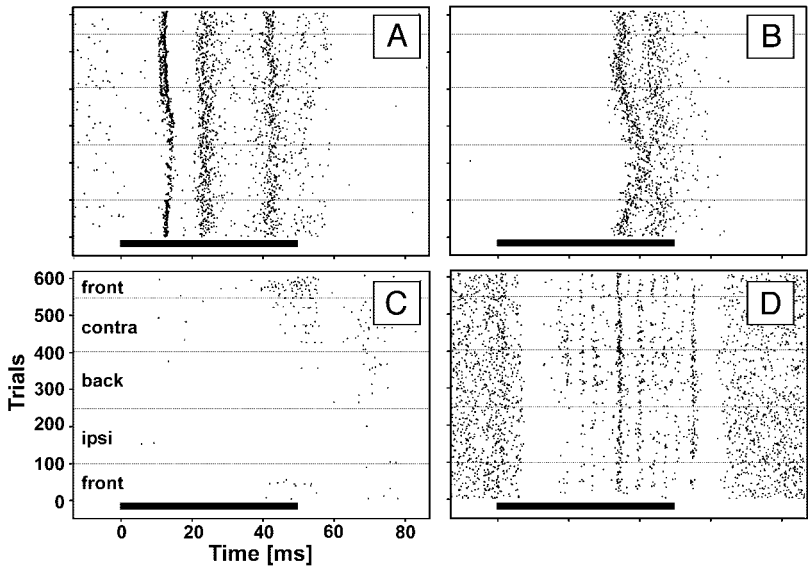

FIG. 4. Spike raster plots. *a*–*d*: spike-time raster plots for 4 sample neurons under white noise stimulation in virtual auditory environment. Spike trains are sorted by trial numbers, starting with *trials 1* to *5* for 5 repetitions of sound direction 0° azimuth/−10° elevation. Hatched lines indicate borders of 3 sectors (front, contra, back, and ipsi). Black bar marks onset and duration of stimulus.

eral and ipsilateral sectors. Neurons tuned to frontal locations were slightly more numerous (56%; Fig. 6*a*) than those tuned to backward directions (44%; Fig. 6*a*). In contrast, the large majority of neurons were tuned to locations in contralateral compared with ipsilateral space (75 vs. 25%; Fig. 6*a*). To examine elevation tuning, the 122 stimulus locations were divided into 3 elevation sectors (around the equator: −10 to 23°; above the equator: 24 to 56°; and extremely high elevations: 57 to 90°). Most of the neurons (60%) preferred elevations near the equator, some neurons (25%) preferred elevations above the equator, and only a few (15%) preferred extremely high elevations (Fig. 6*b*).

Size of spatial receptive fields

To determine the size of a neuron's receptive field to virtual sound sources we measured the maximal extent of their spatial response areas in azimuth and elevation. The receptive field was calculated as follows: the maximum distance intersections of the half-maximum rate isoresponse contour were deter-

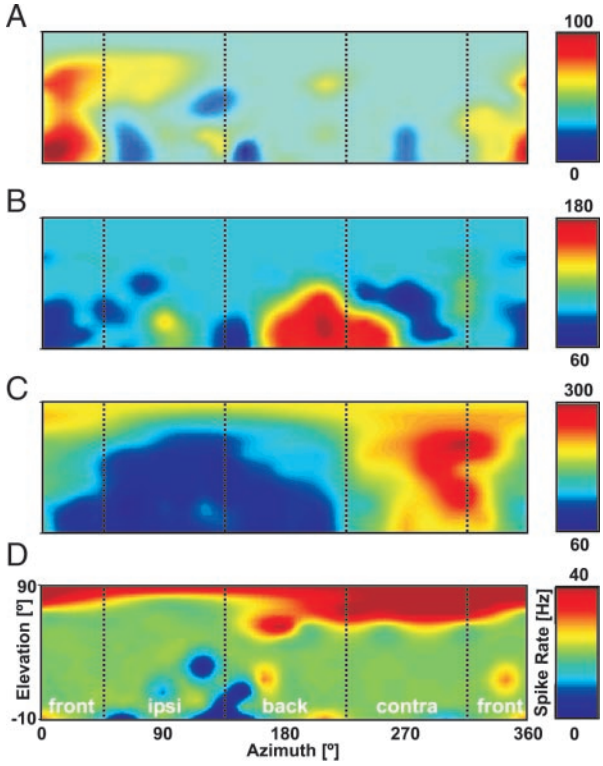

FIG. 5. Spatial responses to virtual sound sources of 4 sample neurons. *a*: this neuron preferred frontal directions; *b*: rear directions; *c*: contralateral directions with mid-to-high elevation; *d*: neuron responded best for very high elevations. Color bar indicates discharge rate after subtraction of spontaneous activity.

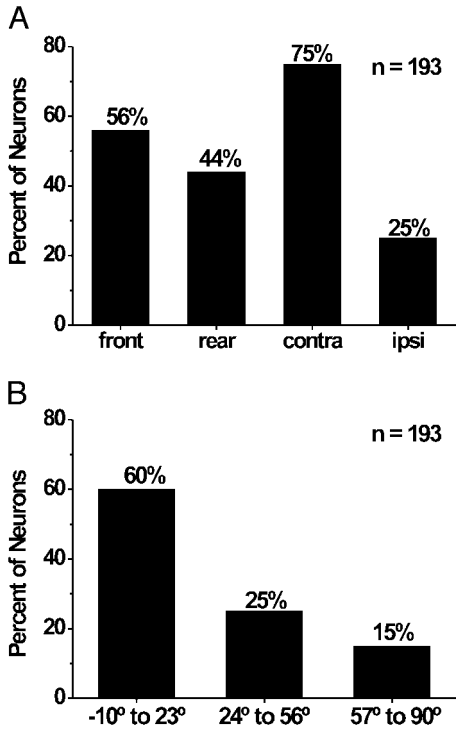

FIG. 6. Distribution of preferred sound source directions of neurons in inferior colliculus (IC). *a*: distribution of best azimuth, sorted by sector (front half and rear half, contralateral and ipsilateral side) of upper hemisphere. *b*: distribution of best elevation. Preferred direction was defined as sound source direction that elicited highest spike rate. In case of a plateau of equal spike rates at neighboring directions, center of plateau was chosen as best direction.

mined. Spontaneous activity was subtracted. Receptive field size in azimuth could be determined for all of the units that showed unfractured RFs ($n = 193$), but those for elevation could be calculated for only 87 units. This was because many neurons ($n = 106$) had a 50% isoresponse contour that was not completely closed at −10° elevation. The average tuning width in azimuth was 60° (interdeciles: 29–138°). For elevation, neurons with small receptive fields dominate (median: 23°, interdeciles: 12–60°), but this may be somewhat biased because elevations less than −10° were not tested. Neurons with a preferred direction close to the median plane (±45° from the midsagittal plane) showed significantly sharper azimuth tuning (median: 50.5°) than neurons with lateral preferred directions (median: 67°, $P < 0.0016$). No significant correlation was found between the sharpness of spatial tuning and either Q_{10dB}-value or "bandwidth" of the tuning curve under tonal stimulation at 80 dB SPL.

Topography of virtual auditory space in the inferior colliculus?

Because other studies have reported a "map" of auditory space in the superior colliculus of the guinea pig (King and Palmer 1983; Sterbing et al. 2002), we examined whether preferred sound source direction was represented topographically in the inferior colliculus. We did not find any topographical representation of auditory space. However, neurons tuned to similar directions were located close to each other. The difference of preferred azimuths of neighboring units was correlated with separation along the electrode track ($P = 0.022$, Spearman rank sum correlation, $n = 56$ tracks). This indicates that neurons with similar best directions tend to be located closer to each other than neurons with different preferred direction. The difference in best elevation was not correlated with track distance. An additional rank variance analysis also failed to reveal any significant relationship between characteristic frequency of the neurons and their preferred direction.

Influence of sound pressure level

A subset of 23 neurons was stimulated with virtual sound sources of different absolute SPL in steps of 20 or 10 dB down to neuronal threshold. We divided the neuronal responses into 3 groups: threshold to 19 dB, 20 to 39 dB, and >40 dB above threshold. For 39% of the neurons, the size of the receptive field, defined as the average of the azimuth angle at half-maximal response, did not change with decreasing SPL by more than 25%. The biggest group of neurons (48%) showed a decrease and 13% an increase of the size of the receptive fields close to threshold. The shift of the preferred direction was usually small (<25°) for suprathreshold SPLs of 20 dB above threshold and higher. For levels closer to threshold (≤19 dB), the shift of the best direction could be substantial, on average 58°. This shift was in most cases directed toward the median plane, suggesting a greater weight of the monaural inputs to the spatial response. This is to be expected for 2 reasons. First, especially for high frequencies, the responses close to threshold reflect the contralateral pinna isoamplification contours because the sound does not reach the far ear. Second, as shown in Fig. 2, the acoustic axis of the guinea pig is located in the frontal sector for a wide frequency range. In summary, the "best directions" remained quite stable over a wide suprathreshold dynamic range (20–60 dB), but the size of the spatial receptive field varied considerably for most neurons. Figure 7*a* shows polar diagrams of the response of an IC neuron for different overall SPLs relative to the neuron's threshold. This neuron is typical for the biggest group of neurons (48%) that shows an increase of the RF size with intensity. Figure 7*b* depicts the average size of the receptive fields for intensity classes with respect to neuronal threshold.

Stimulus bandwidth

Psychoacoustic experiments have shown for a fixed head position that localization degrades as the bandwidth of the sound decreases (Blauert 1996; Hebrank and Wright 1974;

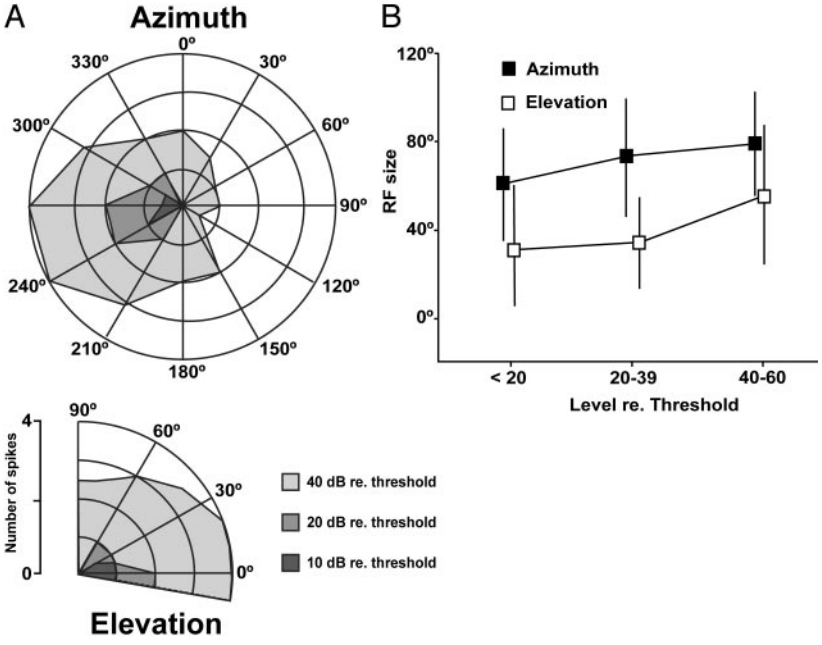

FIG. 7. Influence of overall sound pressure level (SPL). *a*: directional preference of sample neuron stimulated with virtual sound sources of different sound pressure level relative to neuronal threshold. Neuronal activity of neuron is plotted as function of direction of incidence in a polar diagram. *Top panel*: response to different azimuth angles at best elevation. *Bottom panel*: response for different elevations at best azimuth. Note that number of spikes decreased with decreasing SPL, and that spatial selectivity becomes sharper, but preferred direction remained unchanged. *b*: increase of size of receptive field with increasing SPL relative to neuronal threshold ($n = 23$ neurons). Both sizes in azimuth and elevation increase with level.

Roffler and Butler 1968). To examine this effect, we recorded the responses of 46 neurons that were spatially tuned under stimulation with white noise (out of the 80% of the whole sample that were spatially tuned) to noise sources of different bandwidth (white, one octave, 1/3 octave). The center frequency of the one-octave and 1/3-octave bands was chosen according to the characteristic frequency of each neuron. The spectrum level of the stimuli was kept constant. The majority (74%) remained spatially tuned during stimulation with one-octave wide noise. However, with 1/3-octave band stimulation, only 31% remained spatially selective (i.e., they showed hemifield sensitivity or an even smaller receptive field). An example of a neuron that displays decreased spatial tuning with decreasing bandwidth is shown in Fig. 8. For white noise, the neuron displays restricted spatial tuning, for one-octave noise its spatial tuning broadens and becomes hemifield-like, and for a 1/3-octave band noise the spatial tuning disappears and becomes omnidirectional. For one-octave band noise compared with white noise stimulation, the receptive field size remained relatively constant (<25% change) for 58% of the neurons. In 35% of the neurons, the receptive field size became larger, and in 7% became smaller. Of the 58% where the receptive field remained constant in size, only 7% of these showed a change of RF position. For the 31% of the neurons that remained spatially selective to stimulation with a 1/3-octave band noise, the spatial tuning became hemifield-like. In general, the spike rate increased with decreasing bandwidth of the stimuli, suggesting across-frequency inhibitory effects involved in creating small spatial receptive fields.

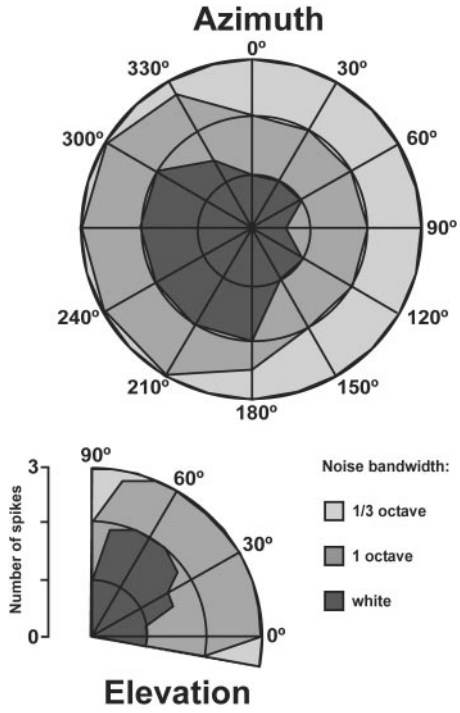

FIG. 8. Influence of stimulus bandwidth. Directional preference of sample neuron stimulated with virtual sound sources of different bandwidths. Neuronal activity of neuron is plotted as function of direction of incidence in a polar diagram. *Top panel*: response to different azimuth angles at best elevation. *Bottom panel*: response for different elevations at best azimuth. Note that number of spikes increased with decreasing bandwidth of noise stimulus. Under stimulation with 1/3 octave band, neuron responded omnidirectionally.

Binaural correlation

Coincidence detection or equivalently cross-correlation is the mechanism by which low frequency neurons achieve their sensitivity to interaural time difference. In contrast, high-frequency neurons are insensitive to ITDs in the fine structure of the signals at each ear because temporal locking to the fine structure of waveforms occurs only at low frequencies. Therefore we tested whether spatial tuning would be altered in low- (<2.5 kHz) and high-frequency (2.5 kHz) neurons, depending on whether the sound was correlated or uncorrelated at the 2 ears. Consistent with our expectations, the spatial tuning of almost all high-frequency neurons (17/19) displayed little if any change when the binaural signal was uncorrelated. Figure 9*b* is a representative example of the minimal effects on the spatial tuning of a high-frequency neuron (6 kHz) when an uncorrelated signal was delivered to the 2 ears. Also consistent with our reasoning, the spatial tuning of most low frequency neurons (11/18) lost their spatial tuning when stimulated with uncorrelated noise. An example of such a neuron (characteristic frequency = 0.8 kHz) is shown in Fig. 9*a*. The restricted spatial tuning under correlated noise becomes almost omnidirectional under stimulation with uncorrelated noise. Of the 7 remaining low-frequency neurons that retained their spatial tuning under uncorrelated noise, only one showed a substantial shift (>45°) of its receptive field. This suggests that ITD sensitivity is not the only mechanism for spatial tuning in these neurons.

Individual versus nonindividual HRTFs

Localization studies on humans using a virtual auditory environment indicate that an individual's own set of HRTFs is necessary for accurate localization. Using another person's HRTFs especially perturbs the perception of frontal and high elevation sound sources (Wenzel et al. 1993). To examine the effects of different HRTFs we compared, in 39 neurons, responses to sounds processed with the animal's own HRTFs with those of another animal's HRTFs (randomly chosen). Figure 10 shows 3 examples of the receptive fields under stimulation with the animal's own versus another animal's virtual sound sources. Figure 10*a* shows the response of a neuron to the noise stimulus convolved with the individual HRTFs (*upper left panel*) and foreign HRTFs (*upper right panel*). This neuron's CF is 12 kHz, and its binaural characteristic is EI (i.e., it receives an excitatory input from the contralateral ear and an inhibitory input from the ipsilateral ear), and thus it might code for ILD. Therefore we plotted the iso-ILD contours for a 1/3-octave band around 12 kHz, as provided by this animal's HRTFs. The neuron appears to follow roughly the −10 dB iso-ILD contour. However, also additional inputs that are not shown cannot be ruled out to further shape this neuron's receptive field. We also calculated the iso-ILD contours for the same frequency band from the foreign HRTFs. Note that the neuronal response reflects some features from these iso-ILD contours, which might explain the altered shape of the receptive field. Another example for a high-frequency neuron is shown in Fig. 10*b*. Only the low-frequency, hemifield-sensitive neuron with EE characteristic (Fig. 10*c*) appears to be unaffected when tested with foreign HRTFs. The iso-ITD contours for these low frequencies did

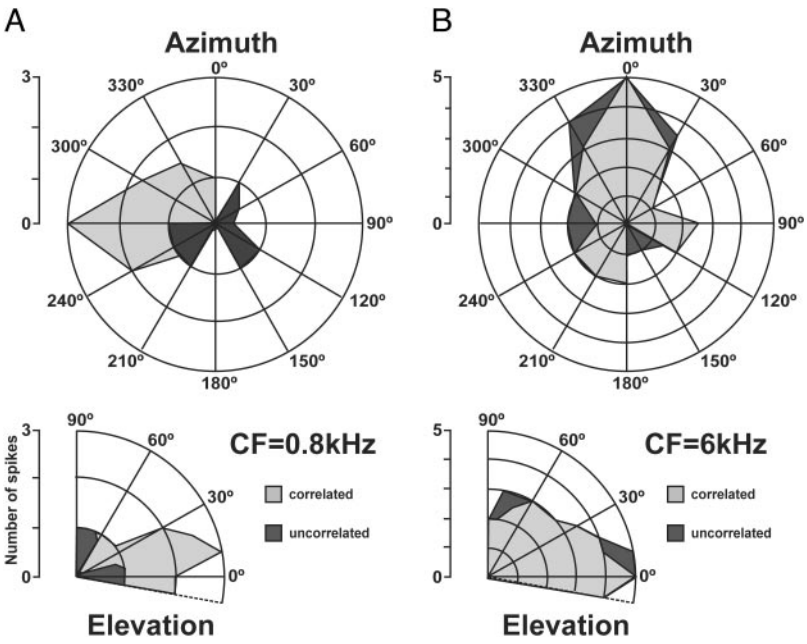

FIG. 9. Influence of binaural correlation. Spatial tuning of 2 sample neurons stimulated with binaurally correlated and uncorrelated noise. Neuronal activity of neuron is plotted as function of direction of incidence in a polar diagram. *Top panels*: response to different azimuth angles at best elevation. *Bottom panels*: response for different elevations at best azimuth. *a*: low-frequency neuron; note that spatial tuning disappeared under stimulation with uncorrelated white noise. *b*: high-frequency neuron; spatial tuning did not significantly change under either condition.

not differ much between the animals (*lower panels*). Over our whole sample ($n = 39$), 64% of neurons exhibited altered spatial tuning when tested with another animal's HRTFs. Another 18% (7/39) responded so weakly that spatial tuning could not be reliably measured using foreign HRTFs. The spatial tuning of the remaining 18% (7/39) did not change appreciably when another animal's HRTFs were used. A change from a restricted to an omnidirectional receptive field was seen in 20% (5/25) of the neurons. In 48% (12/25) the receptive field was fractured, leading to several "best directions" (e.g., Fig. 10*a*). Eight of the 25 (32%) neurons showed a shift of best direction of more than 30°, and for most of these the best direction shifted from front to back. This is consistent with human studies, which show that the number of front/back confusions increases, if another person's set of HRTFs is used (Wenzel et al. 1993; Wightman and Kistler 1989). For the neurons tested with individual versus nonindividual HRTFs, the magnitude of the shift in best direction was on average 45° (interdeciles: 22–105°). The neurons also exhibited an upward shift of best elevation of 15° (interdeciles: −10 to 23.8°). A shift from back to front was observed only once and a shift of the receptive field from one side to the other was never observed. Figure 11 shows typical amounts of the shift of best position for 9 neurons (Fig. 11*a*) or diffraction (Fig. 11*b*) for 5 neurons.

DISCUSSION

We found that: *1*) the vast majority of neurons in the ICc of the guinea pig responds to virtual sound sources; *2*) the entire upper hemisphere of acoustic space is represented in the ICc, but contralateral directions are overrepresented; *3*) the spatial receptive fields are small, and they are often restricted to either the anterior or posterior quadrants; *4*) the representation of sound directions is not topographically organized in the ICc, but neurons with similar best directions tend to be close together; *5*) although the "best direction" of most neurons is not influenced by changes in overall SPL, the size of the spatial receptive field changes for many of them; *6*) the use of individual HRTFs is advantageous to study the spatial tuning of neurons in the guinea pig.

Comparison with studies using free-field stimulation

In many free-field studies on the spatial sensitivity of ICc neurons, near-threshold SPLs were used. The spatial receptive fields obtained using this method essentially reflect the monaural characteristic provided by the pinna (e.g., Fuzessery and Pollak 1985; Moore et al. 1984; Semple et al. 1983), and therefore are unlikely to be the basis for the neural representation of auditory space under natural, suprathreshold conditions. For SPLs well above threshold level, which cover the species-relevant range for communication sounds, most ICc neurons receive binaural input. In other studies using suprathreshold stimulation, ICc neurons seemed to have large spatial receptive fields (Aitkin et al. 1984, 1985; Wenstrup et al. 1988). For example, Aitkin et al. (1984, 1985) found that 39 to 47% of the cat's ICc units were omnidirectional. However, they measured azimuthal directions only at 0–10° elevation. In contrast, we found that many neurons (40%) had a preferred elevation of 24° or higher. If only horizontal directions were measured, we too would have reached a similar conclusion as that of Aitkin and colleagues (1984, 1985) because 50% of the neurons that preferred elevations higher than 24° also showed some low-rate, nonmodulated or only weakly modulated activity for positions along the horizon (e.g., Fig. 5*d*). If those neurons were added to the neurons that were omnidirectional or had large fractured receptive for all tested positions (20%), all the neurons that were "omnidirectional" for azimuths at 0° elevation added up to 36% of the total sample of 242 neurons that responded to the white noise.

We, like others, found that the neurons in the ICc were biased for sounds presented in the contralateral auditory space (Aitkin et al. 1984, 1985; Jen et al. 1987), and could not find a spatiotopic "map" of sound source direction. Even in the barn owl where a spatiotopic map has been demonstrated, such a map could not be demonstrated in the core portion of the ICc

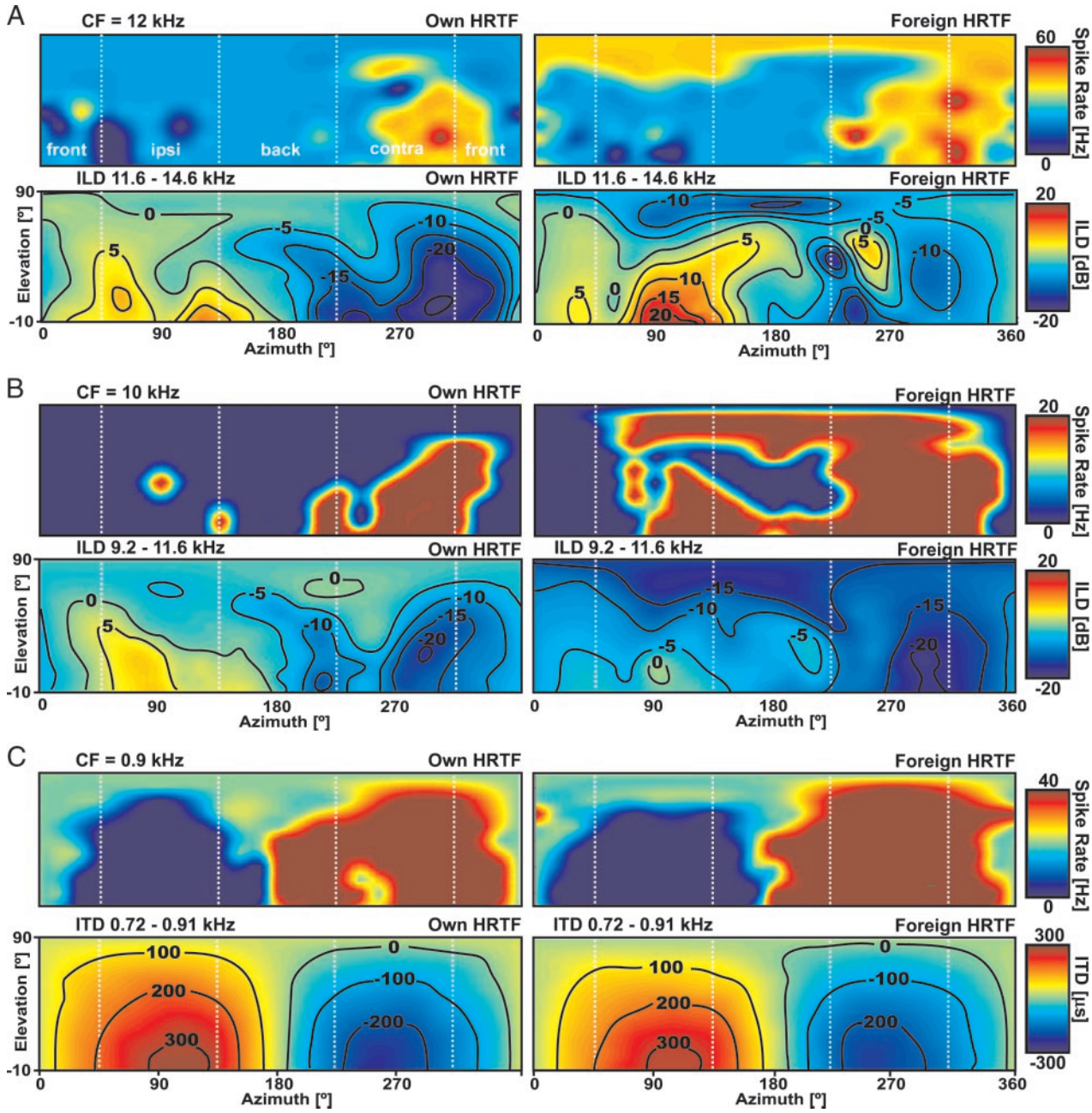

FIG. 10. Own vs. foreign HRTFs. Responses to virtual sound sources of 3 neurons under stimulation using own HRTFs of respective guinea pig (*left top panels*) vs. using HRTF of randomly chosen different individual (*right top panels*). *Bottom panels*: iso-interaural level difference (ILD) or iso-ITD contours calculated from individual HRTFs. *a*: *top panels*: spatial receptive field of this high-frequency neuron broadened especially toward higher elevations, and additional response peaks occurred. Iso-ILD contours for frequency band matching neuron's characteristic frequency show substantial individual differences (*left*: own HRTF; *right*: foreign HRTF), in part reflected by neuronal responses. *b*: response of this high-frequency neuron broadened toward rear and even ipsilateral directions. *c*: response of this low-frequency "hemifield"-sensitive neuron did not change much under either condition. This finding probably reflects similarity of iso-ITD contours of both animals for this low-frequency band.

homolog (nucleus mesencephalicus lateralis dorsalis: Knudsen and Konishi 1978). The lack of a spatiotopic map may be attributed to the restricted number of recorded neurons per guinea pig (mean: 10), with the consequence that interindividual differences could have clouded the results. However, adjacent neurons tended to have similar preferred azimuths. This may be related to the finding that neurons with similar binaural characteristic are clustered in the cat's inferior colliculus (Semple and Aitkin 1979) and that afferents from the contralateral lateral superior olive (LSO) terminate in patches or discontinuous bands in the ICc (Shneiderman and Henkel 1987).

Evidence for convergence of monaural and binaural inputs and across-frequency integration

It is known that in humans, the perceived location of a sound changes as a function of the bandwidth of the signal (Blauert

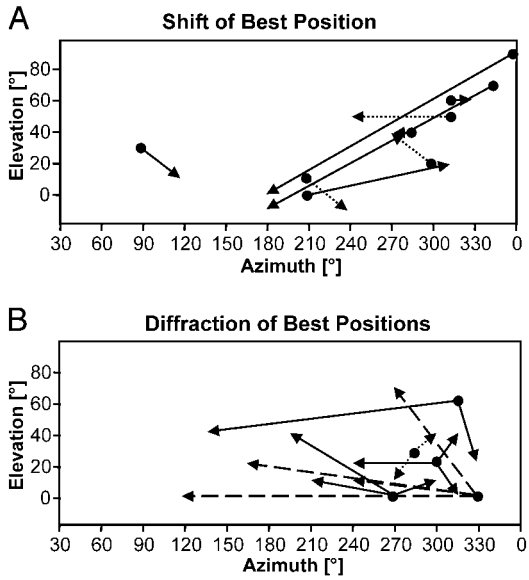

FIG. 11. Own vs. foreign HRTFs. *a*: shift of best position. Circles depict best position under stimulation with own HRTFs. Arrows point to "best position" under stimulation with foreign HRTFs. For clarity, only 9 neurons were included. *b*: diffraction of best positions. Under stimulation with foreign HRTFs many receptive fields have 2 or more maxima of discharge rate. This graph shows diffraction pattern of 5 neuronal receptive fields. All these neurons had only one best position under stimulation with own HRTFs.

1996; Hebrank and Wright 1974; Roffler and Butler 1968). In agreement with the psychoacoustic findings, we found that the spatial tuning of ICc neurons to a broadband signal changed when narrow-band stimuli were used. Furthermore, a neuron's binaural characteristics or its frequency tuning was not related to its spatial tuning features to broadband noise. Thus it appears that the spatial tuning of ICc neurons requires the integration of monaural and binaural cues over a wide frequency range. Whether monaural and binaural information converges on single IC neurons has been the subject of many neuroanatomical and electrophysiological studies (e.g., Oliver 1987, 2000; Oliver and Shneiderman 1991; Oliver et al. 1997; Ramachandran and May 2002). However, many tracer studies support this idea. Overlapping monaural and binaural projections were described for dorsal cochlear nucleus and LSO inputs (Oliver et al. 1997) to the high-frequency area of the IC, as well as for anteroventral cochlear nucleus and medial superior olive inputs to the low-frequency IC of cats (Oliver 1987).

Possible sources for across-frequency integration are intrinsic projections of the IC, or convergent inputs from different brain stem nuclei. For example, Malmierca et al. (1995) showed that distant isofrequency lamina of the guinea pig IC are connected by interneurons. The advantage of across-frequency integration for creating a representation of auditory space was further supported by a model for sound localization (Hartung and Sterbing 2001). This model was based on the neural responses of the present report and the input weights to the model neurons are based on the measured individual HRTFs. The highest input weights were those closest to the characteristic frequency, but additional inputs from distant frequencies enhanced the output activity of the model neuron. Furthermore, convergent binaural (ILD and/or ITD) and monaural inputs produced the closest fit to the measured neuronal responses.

Head-related transfer functions (HRTFs)

We estimated the maximal ITDs by cross-correlating the HRTFs at each ear and found that they ranged $\leq$330 μs as a function of frequency for frequencies lower than about 1,600 Hz. This range of ITDs is considerably greater than that predicted by the interaural distance (about 150 μs; McAlpine et al. 2001). This can be explained by the complicated diffraction patterns of the sound waves traveling around the head and body. The minimum ITD has to be larger than the time difference estimated from the distance between the ears, because the sound travels around the head on different paths, and around the floppy pinna. Because many peaks of ITD functions McAlpine et al. (2001) measured in the guinea pig are well within our measured ITD range, there is no need to postulate that such ITDs are outside the functional range for guinea pigs.

We found, like Carlile and Pettigrew (1987), that the shape of the HRTFs can vary from animal to animal. Moreover, using HRTFs from another animal could alter the spatial tuning of an ICc neuron. Thus using nonindividual HRTFs is problematic. Our finding agrees with human studies that showed that spatial localization is best when the individual's HRTFs are used (Wenzel et al. 1993; Wightman and Kistler 1989). Even when reverberations are added to the nonindividual HRTFs, the incidence of front/back confusions does not decrease (Wightman and Kistler 1996). Studying the auditory cortex of the ferret, Mrsic-Flogel et al. (2001) also found that spatial tuning changed, if nonindividual HRTFs were used. Delgutte et al. (1999) used a set of nonindividual HRTFs measured in a cat and reported that the spatial tuning of IC neurons was broad and omnidirectional. However, they recorded only neurons with a CF higher than 4 kHz because these nonindividual HRTFs did not contain enough energy in the low-frequency range. This leads to the elimination of the low-frequency ITD information, which is very important for sound localization. Similarly, Brugge et al. (1996) used the same nonindividual HRTFs and reported broad spatial receptive fields of neurons in the auditory cortex of the cat. Moreover, many of these neurons had fractured receptive fields. One exception to the problems associated with using nonindividual HRTFs is the barn owl. Comparisons of neural receptive field using individual and nonindividual HRTFs yielded negligible differences (Keller et al. 1998). This may be because the external geometry of the ears in a barn owl is far more consistent in this species compared with those of mammals (e.g., cats and guinea pigs).

To summarize, we found that the entire upper hemisphere of acoustic space is represented in the ICc, but contralateral directions close to the horizon are overrepresented, as previously described also for the superior colliculus of the guinea pig (Sterbing et al. 2002). This is consistent with the finding that the guinea pig has a "visual streak" (Do-Nascimento et al. 1991). The representation of sound directions is not topographically organized in the ICc, but neurons with similar best directions seem to be clustered. The spatial receptive fields are small compared with those found using nonindividual HRTFs, and front–back discrimination can be found on the single-neuron level. The profound asymmetry of the ears as well as different "directional bands" (for review, see Blauert 1996) for front and back positions might be the basis for this front–back discrimination. It is advan-

tageous that individual HRTFs are used, at least for studies on sound localization in the guinea pig.

We thank J. Blauert for the use of the anechoic room and the HRTF measurement equipment, C. Perrey for technical assistance, G. J. Dörrscheidt for online-visualization and stimulation software, and Knowles Electronics and Siemens Audiologische Technik GmbH for providing the miniature microphones.

DISCLOSURES

This work was supported by Deutsche Forschungsgemeinschaft Grants GRK 81/2-96, Ho 450/23-1-347 (to P.I. S. J. Sterbing, and National Institute on Deafness and Other Communication Disorders Grant DC-01366 (to principal investigator, S. Kuwada).

REFERENCES

Aitkin LM, Gates GR, and Phillips SC. Responses of neurons in inferior colliculus to variations in sound-source azimuth. *J Neurophysiol* 52: 1–17, 1984.

Aitkin LM, Pettigrew JD, Calford MB, Phillips SC, and Wise LZ. Representation of stimulus azimuth by low-frequency neurons in inferior colliculus of the cat. *J Neurophysiol* 53: 43–59, 1985.

Blauert J. *Spatial Hearing* (2nd ed.). Cambridge, MA: MIT Press, 1996.

Brugge JF, Reale RA, and Hind JE. The structure of spatial receptive fields of neurons in primary auditory cortex of the cat. *J Neurosci* 16: 4420–4437, 1996.

Cant NB. Identification of cell types in the anteroventral cochlear nucleus that project to the inferior colliculus. *Neurosci Lett* 32: 241–246, 1982.

Carlile S and Pettigrew AG. Directional properties of the auditory periphery in the guinea pig. *Hear Res* 31: 111–122, 1987.

Delgutte B, Joris PX, Litovsky RY, and Yin TCT. Receptive fields and binaural interactions for virtual-space stimuli in the cat inferior colliculus. *J Neurophysiol* 81: 2833–2851, 1999.

Do-Nascimento JL, Do-Nascimento RS, Damasceno BA, and Silveira LC. The neurons of the retinal ganglion cell layer of the guinea pig: quantitative analysis of their distribution and size. *Braz J Med Biol Res* 24: 199–214, 1991.

Fuzessery ZM and Pollak GD. Determinants of sound location selectivity in bat inferior colliculus: a combined dichotic and free-field stimulation study. *J Neurophysiol* 54: 757–781, 1985.

Hammershøi D and Møller H. Sound transmission to and within the human ear canal. *J Acoust Soc Am* 100: 408–427, 1996.

Hartung K, Braasch J, and Sterbing SJ. Comparison of different methods for the interpolation of head-related transfer functions. In: *Spatial Sound Reproduction*. New York: Audio Engineering Society, 1999, p. 319–329.

Hartung K and Sterbing SJ. A computational model of sound localization based on neurophysiological data. In: *Computational Models of Auditory Function*, edited by Greenberg S and Slaney M. Amsterdam: IOS Press, 2001, p. 101–114.

Hebrank J and Wright D. Spectral cues used in the localization of sound sources on the median plane. *J Acoust Soc Am* 56: 1829–1834, 1974.

Inoue J. Effects of stimulus intensity on sound localization in the horizontal and upper-hemispheric median plane. *J UOEH* 23: 127–138, 2001.

Jen PH-S, Sun X, Chen D, and Teng H. Auditory space representation in the inferior colliculus of the FM bat, *Eptesicus fuscus*. *Brain Res* 419: 7–18, 1987.

Jenkins WM and Masterton RB. Sound localization: effects of unilateral lesions in central auditory system. *J Neurophysiol* 47: 987–1016, 1982.

Keller CH, Hartung K, and Takahashi TT. Head-related transfer functions of the barn owl: measurement and neural responses. *Hear Res* 118: 13–34, 1998.

King AJ and Palmer AR. Cells responsive to free-field auditory stimuli in the guinea pig superior colliculus: distribution and response properties. *J Physiol* 342: 361–381, 1983.

Kistler DJ and Wightman FL. A model of head-related transfer functions based on principal components analysis and minimum-phase reconstruction. *J Acoust Soc Am* 91: 1637–1647, 1992.

Knudsen EI and Konishi M. Space and frequency are represented separately in auditory midbrain of the owl. *J Neurophysiol* 41: 870–884, 1978.

Kulkarni A and Colburn HS. Role of spectral detail in sound-source localization. *Nature* 396: 747–749, 1998.

Malmierca MS, Rees A, LeBeau FE, and Bjaalie JG. Laminar organization of frequency-defined local axons within and between the inferior colliculi of the guinea pig. *J Comp Neurol* 357: 124–144, 1995.

McAlpine D, Jiang D, and Palmer AR. A neural code for low-frequency sound localization in mammals. *Nat Neurosci* 4: 396–401, 2001.

Moore DR, Semple MN, Addison PD, and Aitkin LM. Properties of spatial receptive fields in the central nucleus of the cat inferior colliculus. I. Responses to tones of low intensity. *Hear Res* 13: 159–174, 1984.

Mrsic-Flogel TD, King AJ, Jenison RL, and Schnupp JW. Listening through different ears alters spatial response fields in ferret primary auditory cortex. *J Neurophysiol* 86: 1043–1046, 2001.

Oliver DL. Projections to the inferior colliculus from the anteroventral cochlear nucleus in the cat: possible substrates for binaural interaction. *J Comp Neurol* 264: 24–46, 1987.

Oliver DL. Ascending efferent projections of the superior olivary complex. *Microsc Res Tech* 51: 355–363, 2000.

Oliver DL, Beckins GE, Bishop D, and Kuwada S. Simultaneous anterograde labeling of axonal layers from lateral superior olive and dorsal cochlear nucleus in the inferior colliculus of cat. *J Comp Neurol* 382: 215–229, 1997.

Oliver DL and Morest DK. The central nucleus of the inferior colliculus in the cat, *J Comp Neurol* 222: 237–264, 1984.

Oliver DL and Shneiderman A. The anatomy of the inferior colliculus: a cellular basis for integration of monaural and binaural information. In: *Neurobiology of Hearing: The Central Auditory System*, edited by Altschuler RA, Bobbin RP, Clopton BM, and Hoffman DW. New York: Raven, 1991, p. 195–222.

Proakis JG and Manolakis DG. *Digital Signal Processing: Principles, Algorithms and Applications* (2nd ed.). New York: Macmillan, 1982.

Ramachandran R and May BJ. Functional segregation of ITD sensitivity in the inferior colliculus of decerebrate cats. *J Neurophysiol* 88: 2251–2261, 2002.

Rockel AJ and Jones EG. The neuronal organization of the inferior colliculus of the adult cat. I. The central nucleus. *J Comp Neurol* 147: 11–60, 1973.

Roffler SK and Butler RA. Localization of tonal stimuli in the vertical plane. *J Acoust Soc Am* 43: 1260–1266, 1968.

Semple MN and Aitkin LM. Representation of sound frequency and laterality by units in central nucleus of cat inferior colliculus. *J Neurophysiol* 42: 1626–1639, 1979.

Semple MN, Aitkin LM, Calford MB, Pettigrew JD, and Phillips DP. Spatial receptive fields in the cat inferior colliculus. *Hear Res* 10: 203–215, 1983.

Shneiderman A and Henkel CK. Banding of lateral superior olivary nucleus afferents in the inferior colliculus: a possible substrate for sensory integration. *J Comp Neurol* 266: 519–534, 1987.

Sterbing SJ, Hartung K, and Hoffmann K-P. Spatial tuning in the superior colliculus of the guinea pig in a virtual auditory environment. *Exp Brain Res* 142: 570–577, 2002.

Su TK, Woods TM, and Recanzone GH. Effect of intensity on sound localization performance in macaque monkeys. *Soc Neurosci Abstr* 358.10, 2000.

Wenstrup JJ, Fuzessery ZM, and Pollak GD. Binaural neurons in the mustache bat's inferior colliculus. II. Determinants of spatial responses among 60 kHz EI units. *J Neurophysiol* 60: 1384–1404, 1988.

Wenzel EM, Arruda M, Kistler DJ, and Wightman FL. Localization using non-individualized head-related transfer functions. *J Acoust Soc Am* 94: 111–123, 1993.

Wightman FL and Kistler DJ. Headphone simulation of free-field listening. I. Stimulus synthesis. *J Acoust Soc Am* 85: 858–865, 1989.

Young ED, Rice JJ, and Tong SC. Effects of pinna position on head-related transfer functions in the cat. *J Acoust Soc Am* 99: 3064–3076, 1996.